

Effect of Hydrocarbon Chain Length of Amphiphilic Ruthenium Dyes on Solid-State Dye-Sensitized Photovoltaics

Lukas Schmidt-Mende,^{*,†,§} Jessica E. Kroeze,[‡] James R. Durrant,[‡] Md. K. Nazeeruddin,[†] and Michael Grätzel[†]

Laboratory for Photonics and Interfaces, Institute of Chemical Science and Engineering, Swiss Federal Institute of Technology, CH-1015 Lausanne, Switzerland, and Centre for Electronic Materials and Devices, Department of Chemistry, Imperial College, London, Exhibition Road SW7 2AY, U.K.

ABSTRACT

We studied the influence of the hydrophobic hydrocarbon chain length of amphiphilic ruthenium dyes on the device performance in solid-state dye-sensitized solar cells. We found that the dyes with longer hydrocarbon chains gave higher efficiency values when used as a sensitizer in solid-state dye-sensitized solar cells. With increasing chain length, we observed higher currents and open-circuit voltages up to a limiting chain length. We attribute this improvement to the expected larger distance between TiO₂ and the hole conductor, which seems to suppress recombination effectively.

The world energy consumption is rising, which makes the limitations of fossil fuels more and more apparent. Oil prices are as high as ever. If there is no solution to finding a cheap and accessible renewable energy source, then the energy problem will become critical soon.¹ This is certainly one reason that the market of solar cells is one of the fastest growing, despite the fact that the production of conventional silicon solar cells is expensive and also consumes high energy during fabrication.² Therefore, the interests in and the perspectives for cheap alternative solar cells are very high.^{3,4} Solid-state dye-sensitized solar cells are a promising candidate for alternative forms of solar cells. The efficiencies recently surpassed the 4% hurdle, and the performance limit of this type of cell is far from being reached.^{5,6} In addition to the possibility of low production cost, another important advantage over conventional solar cells is the versatile design possibilities, such as production of flexible cells and differently colored devices. The coloration of the device is determined by the dye that is used.

In this study we show that careful engineering of the dye has an immense influence on the device performance. By varying the hydrocarbon chain length of an amphiphilic ruthenium dye (Figure 1a), the efficiency can be improved

significantly. We attribute the importance of the chain length to the role of the dye as a spacer between TiO₂ and the hole conductor. The dye conformation at the dye–hole-conductor interface depends on its chain length. Up to a certain number of hydrocarbon units, the chains seem to stretch out and increase the distance between TiO₂ and the hole conductor. Recombination between electrons and holes is more effectively suppressed by increasing this distance. We assume that up to a certain number of methylene units this distance is correlated to the length of the chain. Our results suggest that a further increase in the chain length does not increase the distance anymore; it is more likely that the C chain collapses and the effective distance and the recombination blocking behavior is reduced again.

Dye-sensitized solar-cells consist of a conducting glass substrate (F-doped SnO₂) that is covered with a dense TiO₂ layer to avoid direct contact with the hole conductor and the SnO₂, which would short-circuit the cell. This smooth compact layer of ~100 nm is deposited by spray pyrolysis⁷ onto the conducting oxide glass (TCO). On top of this layer, a nanoporous TiO₂ film is produced by doctor-blading a TiO₂ paste containing 19-nm anatase particles. After subsequent annealing to 500 °C, the layer has a thickness of ~2 μm. A 0.02 M TiCl₄ solution was applied to the nanocrystalline film overnight at room temperature. Afterward, the substrate was rinsed in distilled water and sintered to 450 °C just prior to dye uptake. A monolayer of the sensitizer was adsorbed onto the film by dipping it into a 3 × 10⁻⁴ M solution of the

* Corresponding author. E-mail: ljs38@cam.ac.uk; phone: ++44 1223 334375; fax: ++44 1223 334373.

[†] Swiss Federal Institute of Technology.

[‡] Imperial College.

[§] Current address: Department of Materials Science and Metallurgy, University of Cambridge, Pembroke Street, Cambridge, CB2 3QZ, U.K.

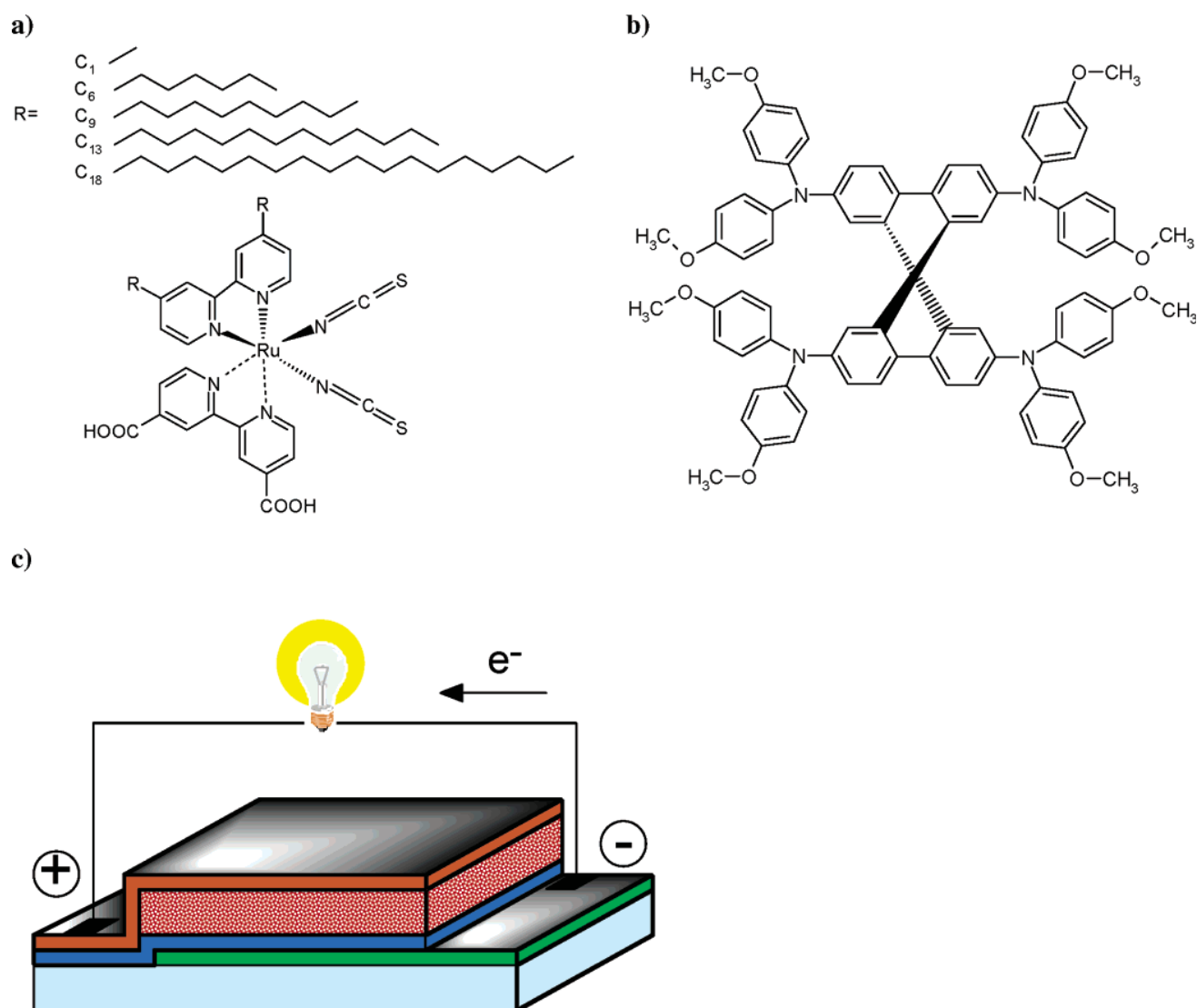


Figure 1. Chemical structures of the dyes with different chain lengths (a) and the hole conductor (b) used for the device preparation are shown next to a schematic of the device structure (c). The devices consist of a glass substrate covered by a conductive transparent electrode (F-doped SnO₂). On top of this a <100 nm compact TiO₂ layer avoids direct contact between the SnO₂ and the hole conductor. The active layer then consists of the ~2- μ m nanoporous TiO₂ layer covered by the dye and filled with the hole conductor. The counter electrode is a 30-nm gold electrode, which is evaporated on top of the hole conductor.

sensitizer dissolved in 1:1 acetonitrile/*tert*-butyl alcohol for ~6 h. The carboxylate groups of the dye used in this study anchor it to the TiO₂ layer. The pores of the TiO₂ layer are then filled with an organic hole-conductor by spin-coating a concentrated (0.17 M) solution of 2,2',7,7'-tetrakis(*N,N*-di-*p*-methoxyphenylamine)-9,9'-spiro-bifluorene (spiro-OMeTAD, see Figure 1c) in chlorobenzene onto the dye-loaded film. The hole-conductor solution was doped with tris(4-bromophenyl)ammoniumhexachloroantimonate (0.3 mM). It also contained additional additives, 13 mM of lithium triflate, and 0.13 M of *tert*-butylpyridine to increase the conductivity of the hole-conducting layer and the open-circuit voltage of the cell.⁸ The devices were finished by thermal evaporation of a gold contact on the hole-conducting layer. A schematic of the cell structure is shown in Figure 1c.

After excitation of the dye with light, electron injection from the dye into the conduction band of the TiO₂ takes place

followed by subsequent hole transfer from the photooxidized dye to the organic hole-conductor, regenerating the dye's original ground state. The charges are collected at the electrodes.^{9,10} The efficiency of the cell very much depends on the selection of the dye. Many different dyes have been used in the dye-sensitized cells using a liquid electrolyte instead of the solid organic hole-conductor.¹¹⁻¹⁶ The cells with the highest efficiencies are usually made with dyes based on ruthenium.¹⁷⁻¹⁹ For solid-state dye-sensitized solar cells, the choice of the dye is even more critical than in the case of liquid electrolyte cells. Here an increase in thickness of the nanoporous TiO₂ layer leads to a higher series resistance in the cell because of the relatively low conductivity of the organic hole-conducting material. Therefore, a dye with high absorption coefficient is needed. Experiments show that a device thickness of a few micrometers gives the highest efficiency values for solid-state solar cells made with

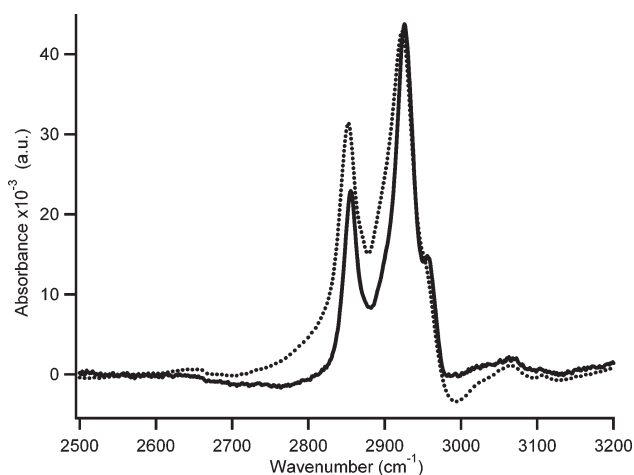


Figure 2. A portion of the normalized ATR-FTIR spectra of the C9 dye complex obtained using a solid sample (dotted line) and adsorbed on a 2- μm thick nanocrystalline TiO_2 film (solid line). The intensity of the adsorbed C9 dye complex is lower than that of the solid sample, which was normalized with respect to 2926 cm^{-1} .

2,2',7,7'-tetrakis-(*N,N*-di-*p*-methoxyphenyl-amine)9,9'-spiro-bifluorene (spiro-OMeTAD) as the hole conductor.⁵ Although the nanoporous TiO_2 layer has a highly increased surface area, usually only a fraction of the incoming light is absorbed in these films. The dyes used in this study are amphiphilic ruthenium dyes with different hydrophobic chain lengths (Figure 1).

The dye complexes have been described in previous studies.²⁰ The ATR-FTIR data of the hydrophobic complexes anchored onto 2- μm -thick nanocrystalline TiO_2 films reveal the mode of adsorption of these dyes onto the TiO_2 surface. The ATR-FTIR spectra of the adsorbed complexes show the presence of carboxylate asymmetric at 1601 $\nu(-\text{COO}^-_{\text{as}})$ and symmetric at 1371 $\nu(-\text{COO}^-_{\text{s}})$ bands, confirming that the carboxylic acid groups are dissociated and involved in the adsorption on the TiO_2 surface. Figure 2 presents infrared spectra of the C9 dye in a solid-state and adsorbed onto a TiO_2 film in the CH stretching mode region. The C9 dye solid sample shows broad bands at 2851, 2922, and 2948 cm^{-1} , which are due to the $\nu(\text{C}-\text{H})$ of the symmetric and asymmetric alkyl chains, respectively.²¹ The antisymmetric vibration mode in the region of 2900 cm^{-1} is a diagnostic for the conformational ordering of the alkyl chain. The bands for the C9 dye adsorbed onto TiO_2 film are observed at 2855, 2926, and 2956 cm^{-1} , which are shifted to higher energy compared to the bands observed for the solid-state C9 dye sample, revealing a higher conformational disorder of C_9H_{19} alkyl chains. In addition to a slight increase of disorder for C_9H_{19} alkyl chains, sharper peaks of the adsorbed complex indicate higher chain rigidity. The superior rigidity with a higher chain disorder suggests possible intra- and/or intermolecular interactions of the alkyl chains, resulting in an aliphatic network.

Photovoltaic devices made with these different dyes showed a significantly different performance (Table 1). As can be seen from Table 1 and Figure 5b, the short-circuit current density as well as the open-circuit voltage increase

Table 1. Device Parameters of Solid-State Dye-Sensitized Solar Cells, Dyed with Amphiphilic Dyes with Different Hydrophobic Hydrocarbon Chain Lengths^a

chain length	current density (mA/cm^2)	open-circuit voltage (mV)	fill factor (%)	efficiency η (%)
C1	5.4	714	59.7	2.3
C6	5.8	712	60.5	2.5
C9	6.3	738	61.3	2.8
C13	6.3	744	66.0	3.1
C18	5.8	718	55.2	2.3

^a In each case, the values represent the mean values of the best three of four cells of two sets of devices for each dye. The device parameters are summarized, including current density, open-circuit voltage, fill factor, and efficiency for devices dyed with the amphiphilic Ru dye with different hydrocarbon chain lengths. All of the devices were prepared in the same way under the same conditions; the only difference can be seen in the difference of the dyes, such that the effect of the dye structure can be clearly detected. The TiO_2 substrates were all soaked for 6 h in the dye solution with the concentration of 3×10^{-4} M in 1:1 acetonitrile/*tert*-butyl alcohol.

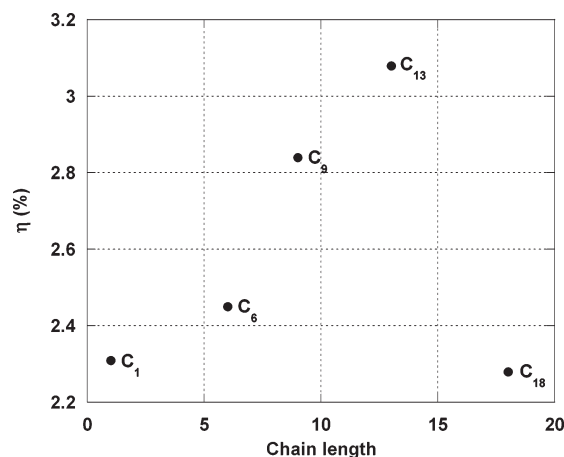


Figure 3. Device efficiency (η in %) vs chain length of amphiphilic dyes with different hydrophobic hydrocarbon chain lengths. Up to the dye with a C13 chain, a linear increase in efficiency can be observed with the increase of the length of the hydrocarbon chain.

significantly with chain length. This leads to a linear increase in device efficiency with chain length (Figure 3). Also, the fill factor ($FF = (V_{\text{OPT}}I_{\text{OPT}})/(V_{\text{OC}}I_{\text{SC}})$, where V_{OPT} and I_{OPT} are current and voltage for maximum power output and I_{SC} and V_{OC} are short-circuit current and open-circuit voltage, respectively) seems to follow this increase. Just for the longest chain, C18, we observe a dramatic decrease in open-circuit voltage, current density, and efficiency. Already the devices with C9 and C13 dye show no difference in the current density, but the open-circuit voltage still increases.

We attribute this behavior to the arrangement of the dye molecules onto the TiO_2 surface, which is strongly influenced by the hole conductor that surrounds the dye. We find an interaction between the hole conductor and dye, which leads to a higher absorption of the dye. The hydrophobic chains of the dyes seem to extend and arrange themselves in the presence of the hole conductor to form an effective spacer between the TiO_2 layer and the hole conductor, which suppresses charge recombination at this interface. At the same time, a close contact between the hydrophobic C chains

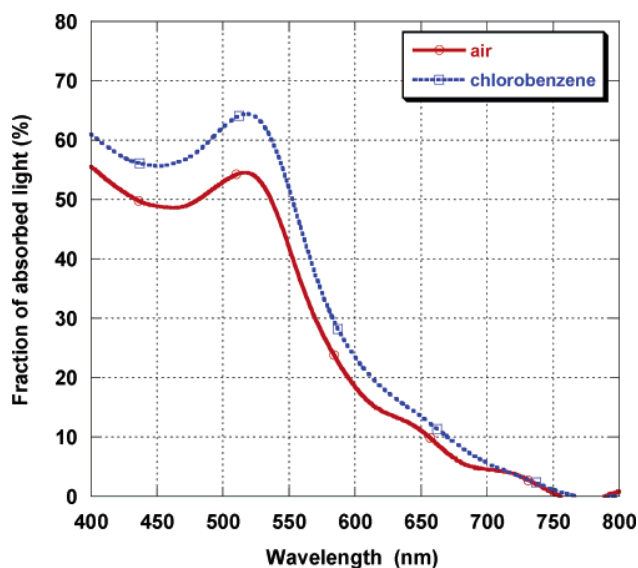


Figure 4. Fraction of absorbed light vs wavelength. The two different curves show an identical 2- μm -thick nanoporous TiO_2 film dyed in both cases with the amphiphilic dye with a C9 chain. In the first measurement, the film was surrounded by air; in the second measurement, the air was replaced with chlorobenzene solution. In both cases, dyed TiO_2 films with identical thicknesses (surrounded by chlorobenzene in the latter case) were used as the background. This increase of the fraction of the absorbed light in the identical film is observed with solvents other than chlorobenzene as well as after contact of the dyed nanoporous TiO_2 layer with the hole conductor.

of the dye and the hole conductor is ensured and enables efficient charge transfer. Therefore, these dyes with their carboxylate groups attached to the TiO_2 surface and their hydrophobic hydrocarbon isolating chains in contact with the hole conductor seem to serve two functionalities: one as the absorber material for the incoming light and the other as a blocking layer between TiO_2 and the hole-conductor layer to avoid charge recombination. The chain length has a strong influence on the blocking behavior of the dye. The longer the chains are, the longer the distance between TiO_2 and the hole conductor seems to be, up to a certain chain-length. The strong interaction between the dye and the hole conductor is supported by UV-Vis data of the dyed TiO_2 films. We find a higher absorption after filling the pores with the hole conductor. This behavior is observed likewise by filling the pores with, for example, chlorobenzene or other solvents. Figure 4 shows the fraction of absorbed light from 400 to 800 nm for a film dyed with C9 dye. The solid curve shows the absorption of the dyed TiO_2 film surrounded by air. A TiO_2 substrate with the same thickness was used as reference. We repeated the same measurement by putting the identical film in chlorobenzene and used a TiO_2 film with the same thickness as blank again, this time surrounded by chlorobenzene. A significant increase in the absorption of the dyed TiO_2 film can be observed, if the dye is surrounded by chlorobenzene, which does not differ from the absorption when surrounded by the hole conductor. We attribute this increase in absorption to conformational changes of the dye, which depends on the length of the hydrocarbon chains and has not been observed previously. Dye N719,²²

which has been used in many cases as a sensitizer for dye-sensitized solar cells, does not show any change in absorption, irrespective of the surrounding media solvent or hole conductor. For our dyes studied here, we observe the highest increase in absorption for the C9 and C13 dye followed by the C6, C1, and C18 dye, successively. Therefore, we assume that the reason of this higher absorption coefficient lies in the extension of the C chains. The longer the chain is, the higher the increase in absorption. Only the decrease of the absorption for the C18 dye does not follow this trend. It is assumed that this very long chain collapses and tends to curl up and does not swell to its full length in the presence of the hole conductor, as seems to be the case for the shorter chains. Therefore, the effective length of the chain does not increase further and the blocking effect is even smaller than that for the dyes with shorter chains. An additional explanation for this strong exception of the C18 dye might lie in the difficulties to purify this dye to the same grade as was done for the other dyes. Therefore, impurities might also lower the device performance.

Dynamic contact angle measurements revealed that the penetration time into a C18 dyed nanoporous TiO_2 film for the spiro-OMeTAD solution is slower than in the case of the other dyes, which showed, within the error of the measurements, very similar dynamics of the contact angles. This is another indication that the very long hydrophobic chain is not stretched, and therefore the hydrophobic character of the chain is not beneficial for the wetting behavior of the hole conductor.

For the C13 dye, the current density does not increase anymore compared to the C9 dye and also the increase in absorption is not higher than that in the case of the C9 dye anymore. This might indicate that already for a chain length of 13 hydrocarbons not all chains are stretched out anymore. More evidence for the assumption that the C13 dye might already have too long of a chain can be seen in the IPCE (incoming photon to current conversion efficiency), which is shown in Figure 5a. Here the order of the devices agrees with the order of the increase in absorption of the different dyes when surrounded by the hole conductor. Even though the IPCE for the C13 devices is slightly lower than that for the C9 device, we observed the same current density under 1 sun for both devices. This can be explained by the nonlinear behavior of the device performance under different illumination intensities. The IPCE measurement is done at relatively low light intensity. The C13 device has its highest efficiency between 50 and 100% sun, whereas for C9 the highest efficiency values were observed for 50% sun and decreased slightly at full sun illumination. Because of the increased open-circuit voltage, the efficiency at 1 sun of the C13 cell is superior to the C9 cell.

In the IPCE data as well as in the absorption data of the films, we observe a modulation of the curves from 600 nm onward, which can be explained by interference effects.

Because of the fact that this increase in absorption does not depend on the surrounding medium (e.g., chlorobenzene, acetonitrile, or hole conductor) a specific interaction with this medium can be excluded. The increase in absorption

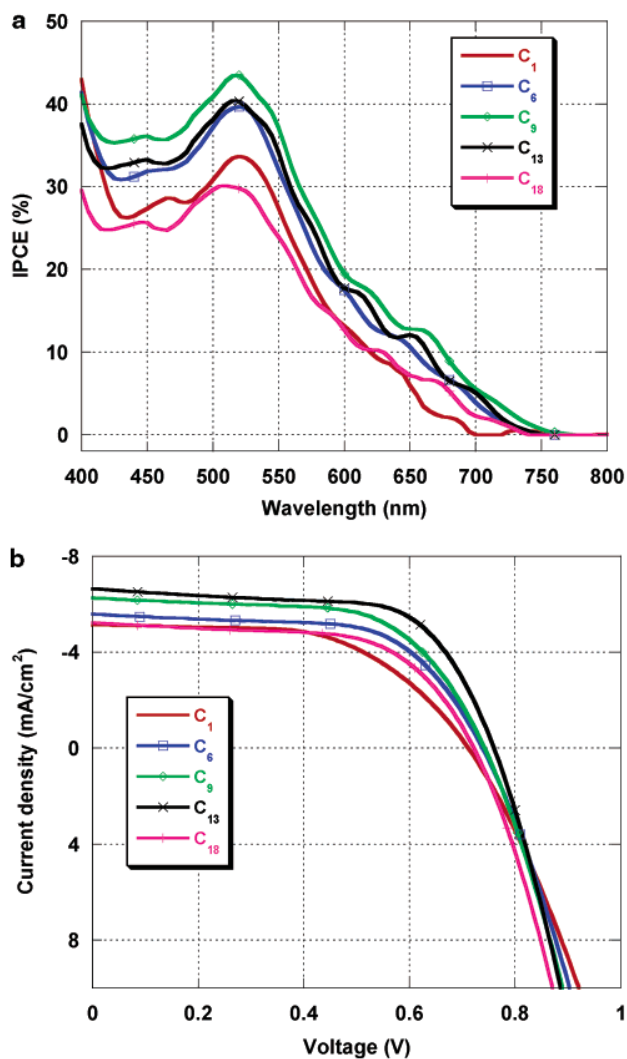


Figure 5. (a) Incoming photon to current conversion efficiency (IPCE) for the dyes with different hydrocarbon chain lengths. The values for the C9 dyed device are the highest followed by C13, C6, C1, and C18, successively. (b) Current–voltage characteristics under 1 sun illumination (AM 1.5 global, 100 W/cm²) for the devices made with these dyes.

depends solely on the dye conformation and depends strongly on the length of the hydrocarbon chain. This increase is not observed for other dyes such as N719, which does not have hydrocarbon chains. Conformation studies of the dye on the TiO₂ surface have to reveal the exact orientation and arrangement of the dye on the TiO₂ surface and therewith the exact nature of the increase in absorption.

Typical transient absorption kinetics, assigned to recombination of e⁻_{TiO₂} with holes on spiro-OMeTAD are shown in Figure 6. All decays were obtained on excitation at 532 nm, close to the absorption maximum of the dye, and probing the photoinduced absorption of TiO₂ electrons and OMeTAD cations at 1000 nm. Data are normalized to the fraction of photons absorbed by the films, enabling the direct comparison of both decay dynamics and charge separation yields. Transient absorption experiments were conducted as reported previously using low intensity (30 μJ cm⁻², 1 Hz, <1 ns) excitation.²⁴

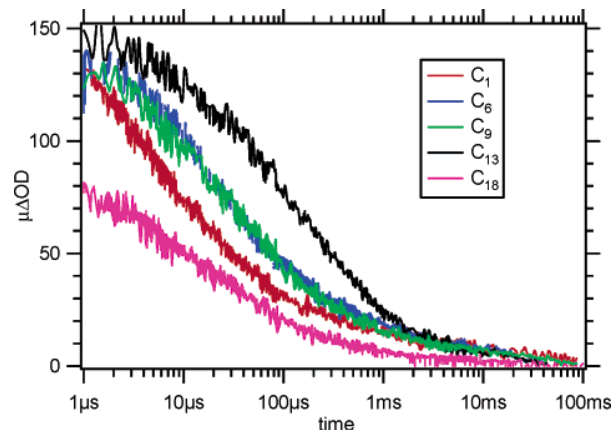


Figure 6. Transient absorption data ($\lambda_{\text{exc}} = 532$ nm, $\lambda_{\text{probe}} = 1000$ nm) monitoring the electron recombination kinetics of nanocrystalline TiO₂ films sensitized with dyes with different alkyl chain lengths in the presence of spiro-OMeTAD.

For the C1–C13 dyes, a retardation of the recombination is observed, with recombination half times, $t_{50\%}$, increasing from 10 to 200 μs, while the charge separation yields (obtained from the initial signal amplitude) remain very similar. This strongly supports our conclusion that the hydrophobic alkyl chains act as an effective spacer between the TiO₂ layer and the hole conductor leading to increasingly suppressed charge recombination at this interface, which is reflected in the increased V_{oc} and overall device performance. For the longest alkyl chain dye, C18, however, we find a strong decrease in recombination time ($t_{50\%} = 20$ μs). This is in agreement with our assumption that this very long chain collapses and does not swell up in the presence of spiro-OMeTAD. As a result, the blocking effect of the C18 alkyl chains is smaller than that for the shorter C6 and C9 chains. In addition, a significant decrease in the charge separation yield for the C18 dye is found. This reduction in signal amplitude is observed for all of the time delays studied (down to ~1 μs), indicating that this reduced yield most probably derives from a reduced efficiency of electron injection from the dye excited state in to the TiO₂ conduction band for this dye, resulting in a decrease of the short-circuit current density. This occurrence of imbalanced charge separation and recombination dynamics is currently the subject of extended studies on liquid-electrolyte and solid-state dye-sensitized solar cells in our laboratories.²³

After optimization of the TiO₂ paste and the doctor-bladed nanoporous TiO₂ layer, the efficiency can be further improved. This has been done previously for the dye with the C9 chain (reported as Z907 dye in the literature).⁵ An efficiency of 4% under a simulated solar spectrum (AM1.5 global) was achieved. The results reported here suggest that a slightly longer hydrocarbon chain length might be advantageous and could lead to even higher efficiencies.

The results suggest that a hydrophobic chain attached to the dye can be used to suppress recombination. A chain length between C9 and C13 seems to be ideal for our system. It is assumed that this is, in general, valid for solid-state devices where recombination is a significant loss mechanism.

In the synthesis of dyes for dye-sensitized solar cells, this should be kept in mind.

We propose another synthetic approach with the same aim. The lengthening of the anchoring groups of the dye would also lead to a longer distance between TiO₂ and the hole conductor. Combined with a hydrophobic chain on the other end, the dye would act more effectively as a spacer and blocking layer between TiO₂ and the hole conductor to avoid recombinational processes. In addition, the prolongation of the structure could be done by extending the π system, which could at the same time also increase the absorption of the dye. Our data suggest that the cell performance improves significantly if the dye acts not only as an absorber but also as an efficient blocking layer.

Acknowledgment. We acknowledge partial funding by the European Commission (FP6 MOLYCELL project, contract no. SES6-CT-2003-502783). L.S.M. thanks the German Research Foundation for Funding (Emmy-Noether Stipendium).

Supporting Information Available: Dynamic contact angle measurements. This material is available free of charge via the Internet at <http://pubs.acs.org>.

References

- (1) Bilgen, S.; Kaygusuz, K.; Sari, A. *Energy Sources* **2004**, *26*, 1119.
- (2) Pietruszko, S. M. *Opto-Electro. Rev.* **2004**, *12*, 7.
- (3) Green, M. A. *Energy Policy* **2000**, *28*, 989.
- (4) Shaheen, S. E.; Ginley, D. S.; Jabbour, G. E. *MRS Bull.* **2005**, *30*, 10.
- (5) Schmidt-Mende, L.; Zakeeruddin, S. M.; Grätzel, M. *Appl. Phys. Lett.* **2005**, *86*, 013504.
- (6) Schmidt-Mende, L.; Bach, U.; Humphry-Baker, R.; Horiuchi, T.; Miura, H.; Ito, S.; Uchida, S.; Grätzel, M. *Adv. Mater.* **2005**, *17*, 813.
- (7) Kavan, L.; Grätzel, M. *Electrochim. Acta* **1995**, *40*, 643.
- (8) Krüger, J.; Plass, R.; Cevey, L.; Piccirelli, M.; Grätzel, M.; Bach, U. *Appl. Phys. Lett.* **2001**, *79*, 2085.
- (9) Bach, U.; Lupo, D.; Comte, P.; Moser, J. E.; Weissörtel, F.; Salbeck, J.; Spreitzer, H.; Grätzel, M. *Nature* **1998**, *395*, 583.
- (10) Bach, U.; Tachibana, Y.; Moser, J.; Haque, S. A.; Durrant, J. D.; Grätzel, M.; Klug, D. R. *J. Am. Chem. Soc.* **1999**, *121*, 7445.
- (11) Ferrere, S.; Zaben, A.; Gregg, B. A. *J. Phys. Chem. B* **1997**, *101*, 4490.
- (12) Hara, K.; Sayama, K.; Ohga, Y.; Shinpo, A.; Suga, S.; Arakawa, H. *Chem. Commun.* **2001**, 569.
- (13) Tokuhisa, H.; Hammond, P. T. *Adv. Funct. Mater.* **2003**, *13*, 831.
- (14) Sayama, K.; Tsukagoshi, K.; Mori, T.; Hara, K.; Ohga, Y.; Shinpo, A.; Abe, Y.; Suga, S.; Arakawa, H. *Sol. Energy Mater. Sol. Cells* **2003**, *80*, 47.
- (15) Horiuchi, T.; Miura, H.; Uchida, S. *J. Photochem. Photobiol., A* **2004**, *164*, 29.
- (16) Schmidt-Mende, L.; Campbell, W. M.; Wang, Q.; Jolley, K. W.; Officer, D. L.; Nazeeruddin, M. K.; Grätzel, M. *ChemPhysChem*, in press.
- (17) Wang, P.; Zakeeruddin, S. M.; Exnar, I.; Grätzel, M. *Chem. Commun.* **2002**, *24*, 2972.
- (18) Wang, P.; Zakeeruddin, S. M.; Humphry-Baker, R.; Moser, J. E.; Grätzel, M. *Adv. Mater.* **2003**, *15*, 2101.
- (19) Wang, P.; Zakeeruddin, S. M.; Moser, J. E.; Nazeeruddin, M. K.; Sekiguchi, T.; Grätzel, M. *Nat. Mater.* **2003**, *2*, 402.
- (20) Nazeeruddin, M. K.; Zakeeruddin, S. M.; Lagref, J. J.; Liska, P.; Comte, P.; Barolo, C.; Viscardi, G.; Schenk, K.; Graetzel, M. *Coord. Chem. Rev.* **2004**, *248*, 1317.
- (21) Snyder, R. G. *J. Chem. Phys.* **1967**, *47*, 1316.
- (22) Krüger, J.; Plass, R.; Grätzel, M.; Matthieu, H. *J. Appl. Phys. Lett.* **2002**, *81*, 367.
- (23) Haque, S. A.; Palomares, E.; Cho, B. M.; Green, A. N. M.; Hirata, N.; Klug, D. R.; Durrant, J. R. *J. Am. Chem. Soc.* **2005**, *127*, 3456.
- (24) Hirata, N.; Lagref, J. J.; Palomares, E. J.; Durrant, J. R.; Nazeeruddin, M. K.; Grätzel, M.; Di Censo, D. *Chem.—Eur. J.* **2004**, *10*, 595.

NL050555Y